Journal of Inclusion Phenomena and Macrocyclic Chemistry (2006) 55:131–149
DOI 10.1007/s10847-005-9029-2

Silicon Analogues of Triarylmethanol Hosts. Inclusion Properties and Host–guest Structures: A Comparative Study

EDWIN WEBER[1,*], WILHELM SEICHTER[1], KONSTANTINOS SKOBRIDIS[2], DIMITRIOS ALIVERTIS[2], VASSILIKI THEODOROU[2], PETRA BOMBICZ[3] and INGEBORG CSÖREGH[4,*]

[1]*Institut für Organische Chemie, Technische Universität Freiberg, Leipziger Str. 29, D-09596, Freiberg/Sachsen, Germany;* [2]*Department of Chemistry, University of Ioannina, GR-45110, Ioannina, Greece;* [3]*Institute of Structural Chemistry, Chemical Research Center, Hungarian Academy of Sciences, P.O. Box 17, H-1525, Budapest, Hungary;* [4]*Department of Structural Chemistry, Arrhenius Laboratory, Stockholm University, S-106 91, Stockholm, Sweden*

(Received: 22 June 2005; in final form: 11 October 2005)

Key words: crystalline inclusion chemistry, inclusion compounds, isostructurality behaviour, supramolecular interactions, triarylmethanol/triarylsilanol hosts, X-ray structure determination

Abstract

The simple triarylmethanol hosts, **2** and **4**, and their silicon analogues, **1** and **3**, have been studied for comparison of the formation of crystalline inclusion compounds. Clathrate formation experiments showed that replacement of the carbinol C atoms in **2** and **4** by Si atoms to give **1** and **3** resulted in a distinct increase of the capability to form inclusion compounds with organic guests, in particular with alcohols. Moreover, the naphthyl derivatives are much more efficient than the phenyl species, irrespective of the carbinol and silanol features. In order to investigate and compare the guest recognition modes and packing relations of hosts **1–4** in their crystalline inclusion compounds, 11 selected co-crystals, namely **1**·DMSO (2:1), **3**·EtOH (1:1), **3**·*i*-PrOH (1:1), **3**·acetone (1:1), **3**·DMSO (1:1), **3**·THF (1:1), **3**·piperidine (1:1), **4**·acetone (1:1), **4**·DMSO (1:1), **4**·1,4-dioxane (1:1) and **4**·benzene (1:1), were studied by X-ray diffraction from single crystals. The survey contains additional 11 crystal structures from the literature and provides a detailed discussion of isostructurality relationships.

Introduction

As a result of their promising uses [1, 2], crystalline inclusion compounds (clathrates) have aroused considerable interest in the past few years [3]. This has given rise to the synthesis of an enormous variety of so-called clathrate hosts, all being capable of the formation of host–guest inclusion compounds in the crystalline state [4]. Depending on the structure of the host compound, remarkable differentiation of guest molecules including constitutional and stereoisomers has been obtained [5, 6]. Developing strategies for the principal host design has rendered good service in this respect [7]. They include motifs such as awkward constitution [8] or coordination assistance of the host molecule [9]. Characteristic examples of compound structures based on these design criteria are the scissor-type [10], the roof-shaped [11], the wheel-and-axle type [5a, 12], the dog-bone or dumb-bell shaped host molecules [13] and others [4]. The vast majority of these host molecules are of purely organic nature, while others, containing inorganic elements such as silicon, phosphorus or arsenic atoms, are relatively rare [12], except for a recent new design of bulky organosilicon hosts [14]. On the other hand, it has been shown that triphenylsilanol (**1**) [15] is a remarkably selective inclusion host for ethanol [16] and higher alcohols, unlike its purely organic counterpart triphenylmethanol (**2**) [17], which is selective for methanol alone [18]. This has stimulated a more thorough comparative study of the inclusion behaviour of this and a related pair of host compounds; the latter ones are tri(1-naphthyl)silanol (**3**) [15, 19] and tri(1-naphthyl) methanol (**4**) [17]. Here we give a detailed report on the inclusion properties of the individual compounds (Scheme 1) and comparatively discuss the inclusion behaviour of the respective silicon or carbon host analogues, including structural study of relevant inclusion compounds. In the course of the present work, 11 crystalline inclusion compounds, namely **1**·DMSO (2:1), **3**·EtOH (1:1), **3**·*i*-PrOH (1:1), **3**·acetone (1:1), **3**·DMSO (1:1), **3**·THF (1:1), **3**·piperidine (1:1), **4**·acetone (1:1),

* Authors for correspondence. E-mail: edwin.weber@chemie.tu-freiberg.de, ics@struc.su.se

4·DMSO (1:1), **4**·1,4-dioxane (1:1) and **4**·benzene (1:1), have been studied by X-ray diffraction on single crystals. The survey comprises additional 11 crystal structures, selected from the literature: **1**·EtOH (4:1) [16], **1**·dioxane (4:1) [15], **2**·MeOH (1:1) [18], **2**·acetone (2:1) [17], **2**·DMSO (2:1) [18], **2**·1,4-dioxane (1:1) [15], **3**·1,4-dioxane (1:1) [15], **3**·toluene (1:1) [19], **3**·*o*-xylene (1:1) [19], **3**·*m*-xylene (1:1) [19] and **3**·*p*-xylene (1:2) [19]. As seen, clathrate structures of hosts **1–3**, containing one of the solvents listed in Tables 1–2 as guest, were selected. Comparison of similar structures provides a detailed discussion of isostructurality relationships [20, 21].

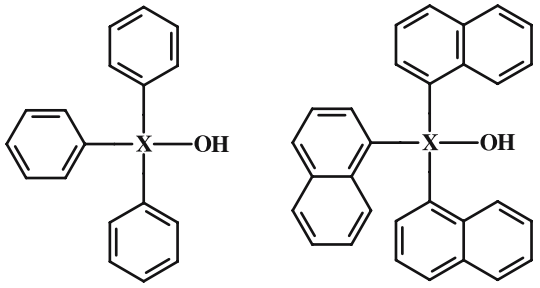

1 X = Si
2 X = C

3 X = Si
4 X = C

Scheme 1.

Experimental

Compounds

The host compounds **1** and **2** were purchased from chemical companies (Aldrich, Fluka). Compound **3** was synthesized according to the literature procedure [19].

*Preparation of tri(1-naphthyl)methanol (**4**)*

To a stirred solution of 1-bromonaphthalene (6.20 g, 30 mmol) in dry diethyl ether (20 mL) under an atmosphere of argon was added *n*-BuLi (2N in *n*-hexane, 16 mL, 32 mmol) at such a rate as to keep the temperature between 0 and 5 °C. When the solution had been stirred for 1 h, a solution of 1-naphthoyl chloride (1.65 g, 10 mmol) in dry diethyl ether (10 mL) was added under the same temperature conditions. The mixture was diluted with additional diethyl ether (20 mL), allowed to warm up to room temperature and was stirred for 2 h at this temperature. Stirring was continued under reflux for 5 h. Then the mixture was cooled with ice and quenched with a saturated aqueous solution of ammonium chloride. The precipitate that formed was collected, washed with water and dried (P_4O_{10}) to yield a first crop (1.5 g, 42%) of **4.** A second crop of **4** (0.7 g, 20%) was obtained from the organic phase, which was separated, washed with water, dried (Na_2SO_4), evaporated and chromatographed (SiO_2 column, Merck, particle size 63–100 μm; eluent: dichloromethane–hexane, 3:1). Total yield 62% colourless solid; m.p. 161–163 °C (ref. [17] m.p. 161–163 °C).

Preparation of crystalline inclusion compounds

Crystals were prepared by recrystallization of the appropriate host compound from a minimum amount of the respective guest solvent. When the solution had stood for 12 h at room temperature, the crystals that had formed were collected and dried (1 h, 15 Torr, room temperature). Host–guest stoichiometric ratios were determined by ^{1}H NMR integration. Data for each compound are given in Tables 1 and 2.

X-ray structure determination

In the course of the present work, 11 crystalline inclusion compounds, namely **1**·DMSO (2:1), **3**·EtOH (1:1), **3**·*i*-PrOH (1:1), **3**·acetone (1:1), **3**·DMSO (1:1), **3**·THF (1:1), **3**·piperidine (1:1), **4**·acetone (1:1), **4**·DMSO (1:1), **4**·1,4-dioxane (1:1) and **4**·benzene (1:1), were studied by X-ray diffraction on single crystals. Reflection intensities were collected at room temperature, using a CAD-4 (Enraf-Nonius) diffractometer for **3**·piperidine (1:1), and STOE Imaging Plate Diffraction System (IPDS) instruments [22] equipped with a conventional X-ray source [for **3**·acetone (1:1)], or a rotating anode (for all

Table 1. Crystalline inclusion compounds (host:guest stoichiometric ratios[a]) of **1** and **2**

Guest solvent	**1**	**2**
Methanol	–	1:1
Ethanol	4:1	–
n-Propanol	1:1	–
n-Butanol	1:1	–
i-Propanol		–
i-Butanol	1:1	–
t-Butanol	1:1	–
Cyclohexanol	1:1	–
n-Propylamine	–	–
Di-*n*-propylamine	–	–
Tri-*n*-propylamine	–	–
i-Propylamine	–	–
t-Butylamine	–	–
Acetone	–	2:1
Dimethyl sulphoxide	2:1	2:1
Dimethylformamide	–	2:1
Acetonitrile	–	–
Tetrahydrofuran	–	–
1,4-Dioxane	4:1	1:1
Piperidine	2:1	1:1
Benzene	–	–
Toluene	–	–
o-Xylene	–	–
m-Xylene	–	–
p-Xylene	–	–
Mesitylene	–	–

[a]Determined by ^{1}H NMR integration.

Table 2. Crystalline inclusion compounds (host:guest stoichiometric ratios[a]) of **3** and **4**

Guest solvent	**3**	**4**
Methanol	–	–
Ethanol	1:1	2:1
n-Propanol	1:1	2:1
n-Butanol	1:1	–
i-Propanol	1:1	1:1
i-Butanol	1:1	–
t-Butanol	1:1	1:1
Cyclohexanol	1:1	2:1
n-Propylamine	1:1	3:2
Di-*n*-propylamine	1:1	1:1
Tri-*n*-propylamine	2:1	–
i-Propylamine	1:1	1:1
t-Butylamine	1:1	1:1
Acetone	1:1	1:1
Dimethyl sulphoxide	1:1	1:1
Dimethylformamide	1:1	1:1
Acetonitrile	1:1	1:1
Tetrahydrofuran	1:1	1:1
1,4-Dioxane	1:1	1:1
Piperidine	1:1	1:1
Benzene	1:1	1:1
Toluene	1:1	1:1
o-Xylene	1:1	1:1
m-Xylene	1:1	1:1
p-Xylene	1:2	1:1
Mesitylene	1:1	1:1

[a]Determined by ^{1}H NMR integration.

the remaining nine structures, see above and Table 3). The net intensities were corrected for Lorentz and polarization effects [22, 23]. Preliminary structure models were deduced by application of direct methods [24]. Some of the non-hydrogen atoms and disorder sites of the guest molecules, and also the hydroxyl hydrogen atoms, were located from difference electron density maps, whereas the carbon-bonded H atoms were given positions calculated from geometric evidence [24]. Full-matrix least-squares calculations on F^2 [24], with anisotropic atomic displacement parameters for all host non-hydrogen positions and selected guest disorder sites, and isotropic ones for the guest minor C and O sites and all the hydrogens, yielded the final structure models shown in Figures 1–3. The guest molecules, in general, exhibit significantly higher mobility than the silanol/carbinol hosts, and in some cases had to be refined with simple distance constraints (Table 3) in order to retain acceptable geometry. Further details of data collection and refinement calculations are given in Table 3.

The crystals of the **3**·*i*-PrOH (1:1) complex proved to be (merohedral) twins. The structure was successfully refined by assuming two domains with orientations *a b c* and *c* –*b a*, respectively, and applying the twin refinement method of the SHELX program system [24, and references therein]. The fractional contributions of both twin components refined to 0.5. Crystals of the **4**·benzene (1:1) complex also proved to be twinned (non-merohedral twins). In this latter case the reflections coming from the two crystal domains had to be resolved. This was done using the software connected with the STOE IPDS instrument [22], but only a limited number of the collected intensities (~50%) could be successfully resolved. Following the data reduction calculations, the two data files were merged after appropriate scaling. However, considerable internal intensity differences [R_{int} = 0.113, $\sigma(R)$ = 0.150; Table 3] were detected in the resulting merged X-ray data, and the refinement calculations converged to relatively high final *R*-values [24] for this **4**·benzene (1:1) complex (Table 3), suggesting moderate quality and comparatively large uncertainty for the observed crystallographic data (F_{obs}^2).

The dimethyl sulphoxide guest in **1**·DMSO (2:1) (Figure 1) is located on a mirror plane, with the oxygen [O(1D)] atom in the special position ½, *y*, ¾. As a consequence, it has two symmetry-related locations, which have the oxygen and the two carbon positions in common and are occupied with equal (50%) probability (Figures 1, 4(a) and 5). Although all included guest molecules, except the non-protic and non-polar benzene, are hydrogen-bonded to the respective host hydroxy function in the present compounds, the guest entities in **3**·EtOH (1:1), **3**·acetone (1:1), **3**·THF (1:1), **4**·DMSO (1:1) and **4**·1,4-dioxane (1:1), exhibited not only dynamic but also static disorder, the latter by occurring in at least two partially occupied disorder positions (Figure 4(b)–(h)). The obtained disorder models of the two crystallographically independent ethanol guests in **3**·EtOH (1:1) are different (Figure 4(b) and (c)), and also those of the two unique DMSO molecules in the **4**·DMSO (1:1) complex (Figure 4(f) and (g)). The LS calculations suggested 58/42 and 55/45% probabilities for the major/minor disorder sites of the ethanol(1) and ethanol(2) molecules (Figure 4(b) and (c)), and 63.2/36.8 and 64.8/35.2% for the DMSO(1) and DMSO(2) sites (Figure 4(f) and (g)), respectively. The corresponding values for the acetone guest in **3**·acetone (1:1) are 54/46% (Figure 4(d)), and those for the 1,4-dioxane molecule in **4**·1,4-dioxane (1:1) are 75/25% (Figure 4(h)). The model of the heavily disordered THF guest in **3**·THF (1:1) (Figure 4(e)) comprises three partly overlapping rings (occurring with approximately 70, 20 and 10% probability, respectively). Concerning the guest H atoms, all partially occupied guest hydrogen sites were included in the final structure models of **1**·DMSO (2:1) (Figure 4(a)), **3**·EtOH (1:1) (Figure 4(b) and (c)) and **3**·acetone (1:1) (Figure 4(d)), whereas, due to the relatively low probability of the minor sites, only the major H disorder sites were realised for the guest molecules in the **3**·THF (1:1) (Figure 4(e)), **4**·DMSO (1:1) (Figure 4(f) and (g)) and the **4**·1,4-dioxane (1:1) complexes (Figure 4(h)).

Table 3. Crystal data and details of the final refinement calculations for compounds **1**·DMSO (2:1), **3**·EtOH (1:1), **3**·*i*-PrOH (1:1), **3**·acetone (1:1), **3**·DMSO (1:1), **3**·THF (1:1), **3**·piperidine (1:1), **4**·acetone (1:1), **4**·DMSO (1:1), **4**·1,4-dioxane (1:1) and **4**·benzene (1:1)

Compound	**1**·DMSO (2:1)	**3**·Et-OH (1:1)	**3**·*i*-PrOH (1:1)
CCDC deposition number	274780	274781	274782
Chemical formula[a]: host	$C_{18}H_{16}OSi$	$C_{30}H_{22}OSi$	$C_{30}H_{22}OSi$
Chemical formula: guest	C_2H_6OS	C_2H_6O	C_3H_8O
Stoichiometry [a]: host:guest	1:0.5	2:2	2:2
Formula weight[a]	315.46	945.27	973.32
Temperature, K	293(2)	293(2)	293(2)
Radiation/λ, Å	MoKα/0.71073	MoKα/0.71073	MoKα/0.71073
Crystal system/space group	Monoclinic/$C2/c$	Monoclinic/$P2_1/n$	Monoclinic/$P2_1/n$
Unit cell dimensions			
a, Å	17.045(2)	24.388(3)	24.253(2)
b, Å	8.682(1)	8.8410(10)	8.9410(10)
c, Å	24.149(3)	23.986(3)	24.264(2)
α, deg	90.0	90.0	90.0
β, deg	96.807(16)	93.569(15)	93.528(10)
γ , deg	90.0	90.0	90.0
V, Å^3	3548.5(10)	5161.7(11)	5251.6(8)
Z[a]	8	4	4
D_c, Mg m^{-3}	1.181	1.216	1.231
μ, mm^{-1}	0.193	0.118	0.118
F(0 0 0)	1336	2000	2064
Approx. crystal size, mm	0.38 × 0.15 × 0.08	0.13 × 0.11 × 0.03	0.28 × 0.24 × 0.04
θ_{max} for collected data, deg	25.83	25.85	25.78
Index ranges min/max h, k, l	−20/20, −9/9, −29/29	−29/29, −10/10, −29/29	−29/29, −10/10, −29/29
Reflections collected	13374	38795	42879
Independent reflections	3222	9870	10022
R_{int}	0.0377	0.1193	0.0872
Refinement method	Full-matrix least-squares on F^2	Full-matrix least-squares on F^2	Full-matrix least-squares on F^2
No. of parameters refined	226	699	697
No. of constraints	0	8	6
R(F) [$I > 2\sigma(I)$]	0.041	0.061	0.045
No. of reflections with $I > 2\sigma(I)$	2494	5206	6360
wR^2[b] (all F^2)	0.112	0.148	0.092
Goodness-of-fit on F^2	1.045	0.976	0.905
Mean/max values of final shift/esd	0.000/0.001	0.000/0.000	0.000/0.001
Largest diff. peak and hole, e Å^{-3}	0.24 and −0.17	0.23 and −0.22	0.31 and −0.23

Compound	**3**·acetone (1:1)	**3**·DMSO (1:1)	**3**·THF (1:1)
CCDC deposition number	274783	274784	274785
Chemical formula[a]: host	$C_{30}H_{22}OSi$	$C_{30}H_{22}OSi$	$C_{30}H_{22}OSi$
Chemical formula: guest	C_3H_6O	C_2H_6OS	C_4H_8O
Stoichiometry[a]: host:guest	1:1	1:1	1:1
Formula weight[a]	484.64	504.69	498.67
Temperature, K	293(2)	293(2)	293(2)
Radiation/λ, Å	MoKα/0.71073	MoKα/0.71073	MoKα/0.71073
Crystal system/space group	Triclinic/P-1	Triclinic/P-1	Triclinic/P-1
Unit cell dimensions			
a, Å	9.1410(10)	9.1260(10)	9.1600(10)
b, Å	13.007(2)	12.8690(10)	13.049(2)
c, Å	12.790(2)	12.8790(10)	12.766(3)
α, deg	62.656(14)	61.865(12)	62.870(18)
β, deg	85.319(15)	87.832(13)	87.835(19)
γ , deg	81.769(15)	83.660(13)	85.824(19)
V, Å^3	1336.6(3)	1325.5(2)	1354.4(3)
Z[a]	2	2	2
D_c, Mg m^{-3}	1.204	1.265	1.223
μ, mm^{-1}	0.116	0.195	0.116
F(0 0 0)	512	532	528

Table 3. Continued.

Approx. crystal size, mm	0.34 × 0.19 × 0.11	0.38 × 0.30 × 0.19	0.32 × 0.19 × 0.09
θ_{max} for collected data, deg	26.18	26.08	25.88
Index ranges min/max h, k, l	−10/10, −16/16, −15/15	−10/10, −15/15, −15/15	−11/11, −15/15, −15/15
Reflections collected	11722	10564	14259
Independent reflections	4920	4848	4855
R_{int}	0.036	0.042	0.063
Refinement method	Full-matrix least-squares on F^2	Full-matrix least-squares on F^2	Full-matrix least-squares on F^2
No. of parameters refined	386	355	360
No. of constraints	6	0	2
R(F) [$I > 2\sigma(I)$]	0.037	0.059	0.049
No. of reflections with $I > 2\sigma(I)$	3029	3319	3260
wR^b (all F^2)	0.092	0.162	0.135
Goodness-of-fit on F^2	0.902	1.06	1.049
Mean/max values of final shift/esd	0.000/0.000	0.000/0.000	0.000/0.000
Largest diff. Peak and hole, e Å^{-3}	0.13 and −0.17	0.31 and −0.29	0.32 and −0.26
Compound	**3**·piperidine (1:1)	**4**·acetone (1:1)	**4**·DMSO (1:1)
CCDC deposition number	274786	274787	274788
Chemical formula[a] :host	$C_{30}H_{22}OSi$	$C_{31}H_{22}O$	$C_{31}H_{22}O$
Chemical formula: guest	$C_5H_{11}N$	C_3H_6O	C_2H_6OS
Stoichiometry[a]: host:guest	1:1	2:2	2:2
Formula weight [a]	511.71	937.13	977.23
Temperature, K	298(2)	293(2)	293(2)
Radiation/λ, Å	CuKα/1.54180	MoKα/0.71073	MoKα/0.71073
Crystal system/space group	Triclinic/P-1	Triclinic/P-1	Triclinic/P-1
Unit cell dimensions			
a, Å	9.4250(10)	8.6960(10)	8.713(2)
b, Å	12.567(3)	13.484(2)	13.438(3)
c, Å	13.026(3)	22.611(3)	22.963(5)
α, deg	114.510(10)	97.023(15)	103.43(3)
β, deg	92.050(10)	97.023(15)	98.38(3)
γ , deg	93.970(10)	92.769(15)	93.54(2)
V, Å^3	1396.9(5)	2560.5(6)	2574.3(10)
Z[a]	2	2	2
D_c, Mg m^{-3}	1.217	1.215	1.261
μ, mm^{-1}	0.947	0.074	0.154
F(0 0 0)	544	992	1032
Approx. crystal size, mm	0.30 × 0.20 × 0.20	0.30 × 0.18 × 0.04	0.26 × 0.13 × 0.03
θ_{max} for collected data, deg	75.19	25.98	26.04
Index ranges min/max h, k, l	0/11, −15/15, −16/16	−10/10, −16/16, −27/27	−10/9, −16/16, −27/28
Reflections collected	6056	20198	16968
Independent reflections	5708	9268	9288
R_{int}	0.024	0.066	0.049
Refinement method	Full-matrix least-squares on F^2	Full-matrix least- squares on F^2	Full-matrix least-squares on F^2
No. of parameters refined	376	704	725
No. of constraints	0	0	14
R(F) [$I > 2\sigma(I)$]	0.063	0.058	0.058
No. of reflections with $I > 2\sigma(I)$	4017	4841	5125
wR^b (all F^2)	0.172	0.145	0.153
Goodness-of-fit on F^2	1.107	0.947	0.943
Mean/max values of final shift/esd	0.000/0.000	0.000/0.000	0.000/0.000
Largest diff. peak and hole, e Å^{-3}	0.31 and −0.33	0.19 and −0.18	0.50 and −0.38
Compound	**4**·dioxane (1:1)	**4**·benzene (1:1)	
CCDC deposition number	274789	274790	
Chemical formula[a]: host	$C_{31}H_{22}O$	$C_{31}H_{22}O$	
Chemical formula: guest	$C_4H_8O_2$	C_6H_6	
Stoichiometry[a]: host:guest	1:1	1:1	
Formula weight[a]	498.59	488.59	

Table 3. Continued.

Temperature, K	293(2)	293(2)
Radiation/λ, Å	MoKα/0.71073	MoKα/0.71073
Crystal system/space group	Triclinic/*P*-1	Triclinic/*P*-1
Unit cell dimensions		
a, Å	8.9570(10)	8.792(2)
b, Å	12.468(2)	12.460(3)
c, Å	13.081(2)	13.457(4)
α, deg	63.728(17)	116.58(3)
β, deg	89.691(18)	91.61(3)
γ , deg	87.120(19)	92.24(3)
V, Å^3	1308.0(3)	1315.7(6)
Z[a]	2	2
D_c, Mg m^{-3}	1.266	1.233
μ, mm^{-1}	0.079	0.072
F(0 0 0)	528	516
Approx. crystal size, mm	0.30 × 0.11 × 0.03	0.27 × 0.17 × 0.06
θ_{max} for collected data, deg	25.91	25.93
Index ranges min/max *h*, *k*, *l*	−10/10, −15/15, −15/16	−10/10, −15/15, −16/16
Reflections collected	11782	4404
Independent reflections	4510	2470
R_{int}	0.033	0.114
Refinement method	Full-matrix least-squares on F^2	Full-matrix least-squares on F^2
No. of parameters refined	398	371
No. of constraints	14	6
R(F) [$I > 2\sigma(I)$]	0.057	0.099
No. of reflections with $I > 2\sigma(I)$	3081	1266
wR^2[b] (all F^2)	0.146	0.234
Goodness-of-fit on F^2	1.073	1.093
Mean/max values of final shift/esd	0.000/0.000	0.000/0.000
Largest diff. peak and hole, e Å^{-3}	0.23 and −0.19	0.20 and −0.19

[a]Chemical formula, host–guest stoichiometry, formula weight and multiplicity (*Z*) refer to the crystallographic asymmetric unit.
[b]The weights of the F^2 values were assumed as $w = [\sigma^2(F^2) + (\mathbf{c_1}\cdot P)^2 + (\mathbf{c_2}\cdot P)]^{-1}$, where $P = (F_o^2 + 2F_c^2)/3$; and the constants $\mathbf{c_1}$ and $\mathbf{c_2}$ had the values 0.0660 and 0.500 for **1**·DMSO (1:1), 0.0650 and 0.0 for **3**·EtOH (1:1), 0.0400 and 0.0 for **3**·*i*-PrOH (1:1), 0.0470 and 0.0 for **3**·acetone (1:1), 0.0470 and 1.560 for **3**·DMSO (1:1), 0.078 and 0. 0 for **3**·THF (1:1), 0.073 and 0.520 for **3**·piperidine (1:1), 0.0678 and 0.0 for **4**·acetone (1:1), 0.0835 and 0.0 for **4**·DMSO (1:1), 0.0845 and 0.0 for **4**·1,4-dioxane (1:1), and 0.1100 and 0.0 for the **4**·benzene (1:1) inclusion crystal.

Results and discussion

Synthesis

While the host compounds **1** and **2** were used as commercially obtained, **3** and **4** were synthesized compounds. The silanol **3** was prepared by strictly following the literature description [19], but the method presently employed for synthesis of carbinol **4** is a substantial modification of the literature procedure [17]. As for the latter case, a subsequent finding is that when using the reaction between 1-bromonaphthalene and 1-naphthoyl chloride via the Grignard route [25], most of the product obtained is 1′-(1,2′-binaphthyl) 1-naphthyl ketone, with **4** as a by-product only. The ketone structure has been established by single-crystal X-ray determination [26]. This unexpected behaviour may be ascribed to a competing Michael-type reaction of the Grignard reagent with the intermediate di-1-naphthyl ketone, due to steric hindrance. However, when making use of the analogous organolithium reaction between 1-naphthyllithium (prepared from 1-bromonaphthalene and *n*-butyllithium) and 1-naphthoyl chloride, the desired carbinol **4** is formed as the main product in 62% yield, with the above ketone as by-product.

The crystalline inclusion compounds (Tables 1 and 2) were prepared from a saturated host solution in the respective guest solvent as specified in the experimental section.

Inclusion properties

In order to show the inclusion properties clearly and to ensure a complete comparison, all host compounds **1–4** were tested with the same range of solvents (Tables 1 and 2). These include alcohols and amines of different molecular sizes and shapes, dipolar aprotic compounds of different polarities, heterocycles of different ring sizes and with different numbers and types of heteroatoms, as well as apolar aromatic hydrocarbons that differ in the degree of substitution and the orientation of substituents. The ability of **1** and **2** to form inclusion compounds is evident from Table 1, which specifies 15 different

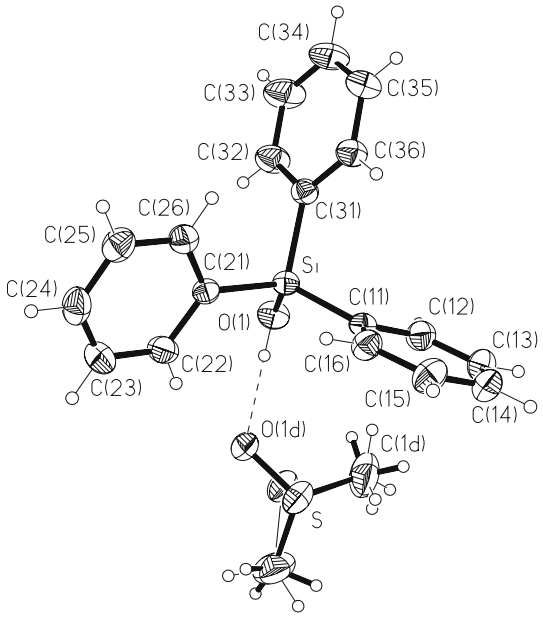

Figure 1. Perspective view of the 1:1 host–guest unit of **1**·DMSO (2:1) including the numbering scheme of unique atom positions. The displacement ellipsoids of the non-hydrogen atoms and disorder sites are drawn at 30% probability level. The DMSO guest molecule may occur in either of two symmetry-related disorder sites with equal probability. One of these two sites has bonds drawn with thinner lines. The host–guest hydrogen bond interaction is indicated by a dashed line.

species, while Table 2, showing a list of 47 different species, demonstrates the inclusion behaviour of **3** and **4.**

This already allows drawing a first distinction between **1** and **2** *versus* **3** and **4**, where **3** and **4** are highly superior in numbers of inclusion compounds formed. The general conclusion from this fact is that the naphthyl derivatives are much more effective inclusion hosts than the basic phenyl-containing compounds, irrespective of the carbinol and silanol features. However, when making a comparison between the carbinol and silanol derivatives, the findings are that in the phenyl case (Table 1) the silanol (**1**) is more efficient in inclusion formation than the carbinol (**2**), but in the naphthyl case (Table 2) the host compounds (i.e. **3** and **4**) are rather equal in effectiveness, with only a very small excess in numbers of inclusion compounds for the silanol (**3**).

On going into details (Table 1), it is found that the silanol **1** principally differs from the carbinol **2** in the broad formation of inclusion compounds with alcohols, whereas **2** yields only a 1:1 inclusion compound with methanol and fails totally with alcohols of higher molecular weight, demonstrating extraordinary inclusion behaviour [17, 18]. Surprisingly enough, **1** shows an exactly opposite behaviour, forming no crystalline inclusion compound with methanol, but only with higher alcohols starting from ethanol. The inclusion compound of **1** with ethanol has the unusual host:guest stoichiometric ratio 4:1 [16], while all other alcohol inclusions of **1** show 1:1 stoichiometric ratios. This rare 4:1 host:guest ratio is also typical of the inclusion compound of **1** with 1,4-dioxane, in contrast to the 1:1 1,4-dioxane inclusion of **2** [15]. The only inclusion compounds of **1** and **2** corresponding in stoichiometric ratio (2:1) are the inclusion compounds with dimethyl sulphoxide, while those with 1,4-dioxane and piperidine differ.

A more particular consideration of the inclusion properties of the naphthyl-substituted silanol (**3**) and carbinol (**4**) hosts (Table 2) reveals a few differences, largely limited to the inclusions of alcohols and amines, whereas the inclusions otherwise generally show correspondence. Excepting the few cases of solvents that yielded inclusion compounds with **3** but failed with **4**, such as *n*-butanol, *i*-butanol and tri-*n*-propylamine, another difference is in the host:guest stoichiometric ratio, where **3** is in favour of the guest, which is noticeable for the inclusion compounds with ethanol, *n*-propanol cyclohexanol, *n*-propylamine and *m*-xylene. A further remarkable finding is that neither **3** nor **4** gave an inclusion compound with methanol, in contrast to **2** but in accordance with **1.** Nevertheless, in a broad comparison, the striking differences between the silanols **1** and **3** are revealed in the inclusion behaviour with amines and aromatic hydrocarbons, while the carbinols **2** and **4** clearly differ in the inclusion properties with alcohols, amines and aromatic hydrocarbons.

In view of the features discussed above, the crystal structures of 11 relevant inclusion species were investigated (Table 3), and were compared with related ones from the literature [15, 16, 17, 18, 19].

Structural studies

The crystallographic asymmetric units of 11 inclusion compounds, namely **1**·DMSO (2:1), **3**·EtOH (1:1), **3**·*i*-PrOH (1:1), **3**·acetone (1:1), **3**·DMSO (1:1), **3**·THF (1:1), **3**·piperidine (1:1), **4**·acetone (1:1), **4**·DMSO (1:1), **4**·1,4-dioxane (1:1) and **4**·benzene (1:1), are presented in Figures 1–3. Disorder models of relevant guest components are shown in Figure 4, and the packing arrangements are illustrated in Figures 5–10. Parameters of hydrogen-bond type interactions are given in Table 4.

X-ray diffraction analyses indicated structural relationship between solid inclusion compounds of the trinaphthyl-substituted silanol and methanol molecules, i.e. of hosts **3** and **4**. Some co-crystals of the related triphenyl-substituted hosts, namely **1** and **2**, also resemble each other more or less. In order to estimate the degree of isostructurality [20, 21], the cell similarity indices (Π) of the crystallographic unit cells, and also the isostructurality [I(s)] and molecular isometricity indices [I(m)] of the host frameworks were calculated for selected pairs of compounds. They are presented in Tables 5–9.

Comparison of the unit cell parameters in the two crystal structures leads to the *cell similarity index* Π [20, 21]. In the event of great similarity, Π has a value close to zero. On the other hand, in the calculation of the *isostructurality index* [I(s)] [20, 21], both the differences in molecular geometry and the positional differences (ΔR_i) caused by rotational and/or translational opera-

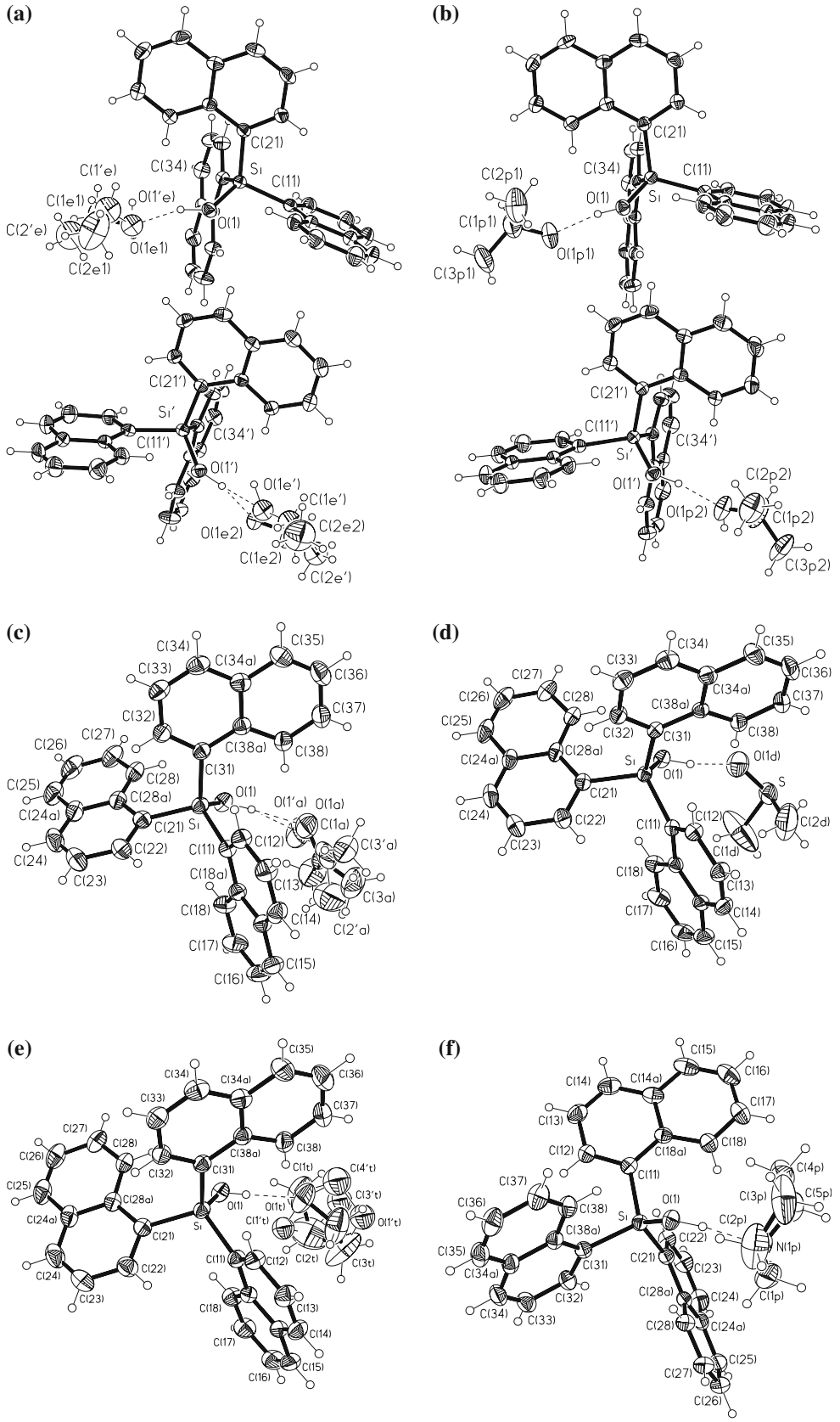

Figure 2. Perspective views of the crystallographic asymmetric units of the inclusion compounds of **3**: (a) **3**·EtOH (1:1), (b) **3**·*i*-PrOH (1:1), (c) **3**·acetone (1:1), (d) **3**·DMSO (1:1), (e) **3**·THF (1:1), (f) **3**·piperidine (1:1). Unique non-hydrogen positions are labelled in (c)–(f), whereas only selected positions are labelled in (a) and (b), the latter ones containing two symmetry-independent host–guest units. The displacement ellipsoids of the non-hydrogen atoms and disorder sites are drawn at 30% probability level. Bonds to minor disorder sites in (a), (c) and (e) are drawn with thinner lines, and dashed lines in (a)–(f) indicate host–guest hydrogen bond interactions.

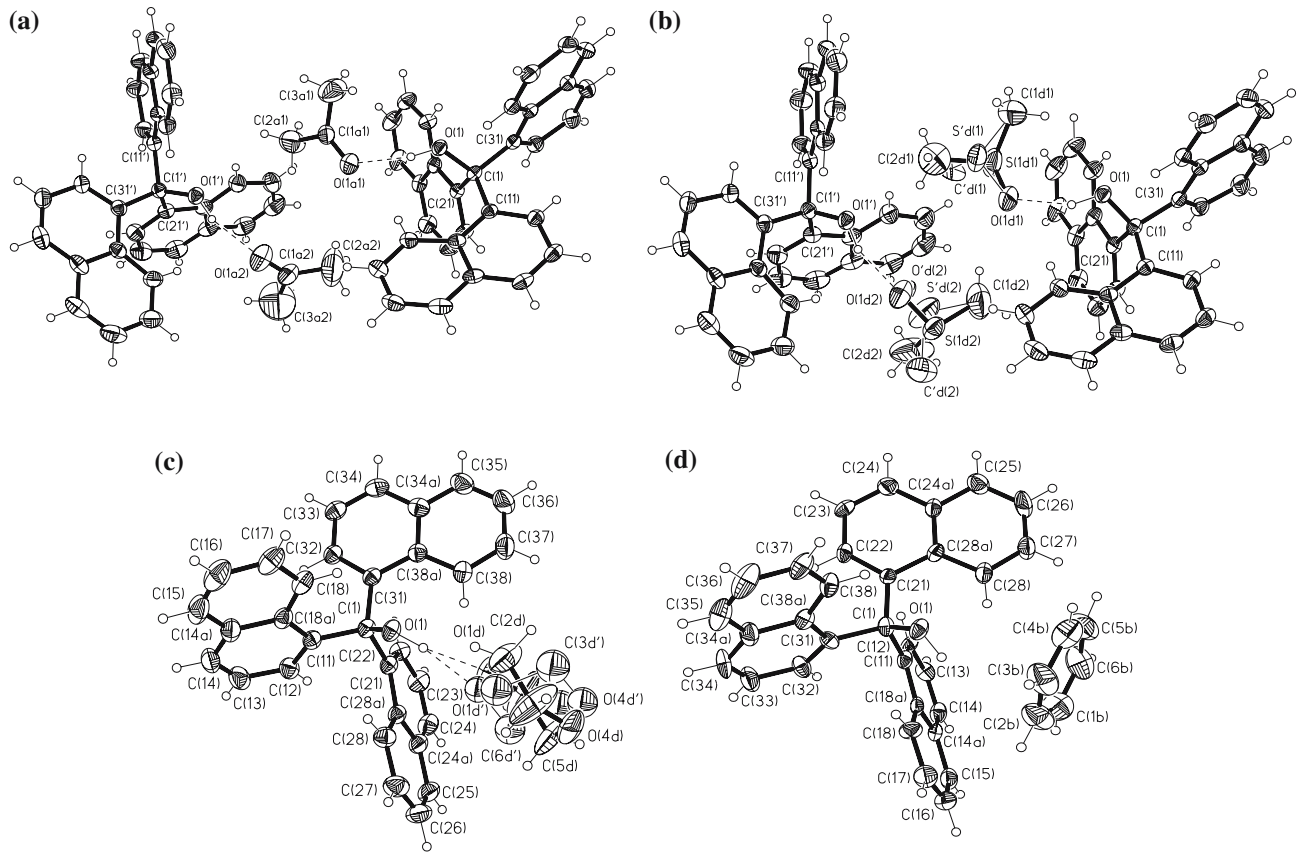

Figure 3. Perspective views of the crystallographic asymmetric units of the inclusion compounds of **4**: (a) **4**·acetone (1:1), (b) **4**·DMSO (1:1), (c) **4**·1,4-dioxane (1:1), (d) **4**·benzene (1:1). Unique non-hydrogen positions are labelled in (c) and (d), whereas only selected positions are labelled in (a) and (b), the latter ones containing two symmetry-independent host–guest units. The displacement ellipsoids of the non-hydrogen atoms and disorder sites are drawn at 30% probability level. Bonds to minor disorder sites in (b) and (c) are drawn with thinner lines, and dashed lines in (a)–(c) indicate host–guest hydrogen bond interactions.

tions are taken into account. At the same time, using refined ΔR_i values from a full or partial least-squares fitting of the positions occupied by corresponding atoms in the two superimposed structures leads to a new index, termed *isometricity index* [*I*(m)] [20, 21], which is seen as a direct measure of the degree of approximate isomorphism of the two compared molecules or associates. In the case of inclusion compounds, calculation of the *I*(m) values for the host molecules may give information about the effect of the different guest molecules on the host conformations and/or host frameworks. The *I*(s) and *I*(m) values in the present study were calculated using all unique non-hydrogen atom positions of the involved host molecules.

Comparison of two solid inclusion compounds of the triphenyl silanol host (**1**) from the literature, **1**·EtOH (4:1) [16] (with the CCDC ref. code SITKEL [27]) and **1**·1,4-dioxane (4:1) [15] (ref. code JODYAC [27]), shows, that both complexes exhibit triclinic (*P*-1) crystal symmetry and 4:1 host–guest stoichiometry. Four hosts and one guest molecule form each H-bonded associate through host–guest and also host–host hydrogen bonds in both crystals, but the topologies of the H-bonding schemes and the shapes of the H-bonded units are different. Accordingly, an asymmetric closed loop of H-bonds [**R** $^{5}_{5}$**(10)**] [28, 29] is created by five OH functions of four host and one guest molecules in **1**·EtOH (4:1) [16], whereas each 1,4-dioxane O atom is acceptor of a hydrogen bond from a H-bonded host dimer in **1**·1,4-dioxane (4:1) [15], thus leading to an H-bond pattern with the graph-set notation [**D** $^{4}_{4}$ **(12)**] [28, 29]. Also the unit cells differ in both shape and size, containing four H-bonded 4:1 host–guest associates with ethanol [SITKEL], but only two with dioxane guest [JODYAC]. A crystallization experiment of host **1** from DMSO solution yielded a complex with 2:1 host:guest stoichiometry (Table 1), thus suggesting different organization for this compound, as compared with previous literature data [30, 31]. The X-ray diffraction study of the **1**·DMSO (2:1) complex indicated monoclinic (*C*2/*c*) crystal symmetry, and H-bonded associates, each formed by two hosts and one guest molecule *via* two symmetry-related host–guest (O)H···O bonds (Table 4, Figure 5). Actually, this kind of double-acceptor guest-molecule pattern with the graph-set descriptor [**D** $^{2}_{2}$**(5)**] [28, 29], has been recognized previously as a characteristic supramolecular motif of DMSO complexes [32, 33]. The various hydrogen bonded associates in each of these three studied crystals of host **1** are then held together by weaker van der Waals forces so as to yield pocket-like (aediculate-type) [34] host frameworks. The realized packing arrangements are, however, different.

After finishing the manuscript the authors became aware of a recent publication of the structure of the **1**·DMSO (2:1) complex, based on low temperature (120 K) data [35].

Four crystal structures have been selected from the literature with the closely related triphenylmethanol host (**2**), containing acetone [**2**·acetone (2:1), JARRUP02] [17, 27], DMSO [**2**·DMSO (2:1), JARROJ] [18, 27], 1,4-dioxane [**2**·1,4-dioxane (1:1), JODXUV] [15, 27] and methanol [**2**·MeOH (1:1), JARRID] [18, 27] as guest. Inspection of the crystal data suggests that these four compounds may be divided into two pairs of related crystals, namely JARRUP/JARROJ and JODXUV/JARRID, respectively (Table 5). The acetone- and the DMSO-containing complexes have 2:1 host:guest stoichiometry and show monoclinic ($C/2c$) crystal symmetry, whereas those containing 1,4-dioxane and methanol as guest, have 1:1 host:guest ratio and triclinic crystal symmetry (P-1). Indeed, comparison of the unit cell dimensions yielded cell similarity indices (Π) with relatively low values for both pairs of compounds (Table 5). Moreover, the host molecule **2** seems to exhibit comparable conformations in its different inclusion crystals, as shown by the isometricity indices, I(m), comparing all the 20 non-hydrogen atoms in each host. Nevertheless, inspection of the crystal structures revealed significant variations in the location of the molecules within the unit cells, and also in the host:guest recognition modes. One important difference is, e.g., that in spite of the same host:guest ratio, the H-bonded unit in **2**·1,4-dioxane (1:1) consists of one host and one guest, linked together *via* a single O(H)···O bond, whereas in **2**·MeOH (1:1) 2:2 host–guest associates are created through closed loops of hydrogen bonds, each with the graph-set notation [$\mathbf{R}\ ^{4}_{4}\mathbf{(8)}$] [28, 29]. Accordingly, despite the apparent similarity, there is no isostructural relationship between the compared inclusion compounds of host **2**.

Comparison of the related co-crystals of hosts **1** and **2** indicates similarities as well as distinct differences. For example, the investigated alcoholic inclusion crystals, namely **1**·EtOH (4:1) [16] and **2**·MeOH (1:1) [18], exhibit

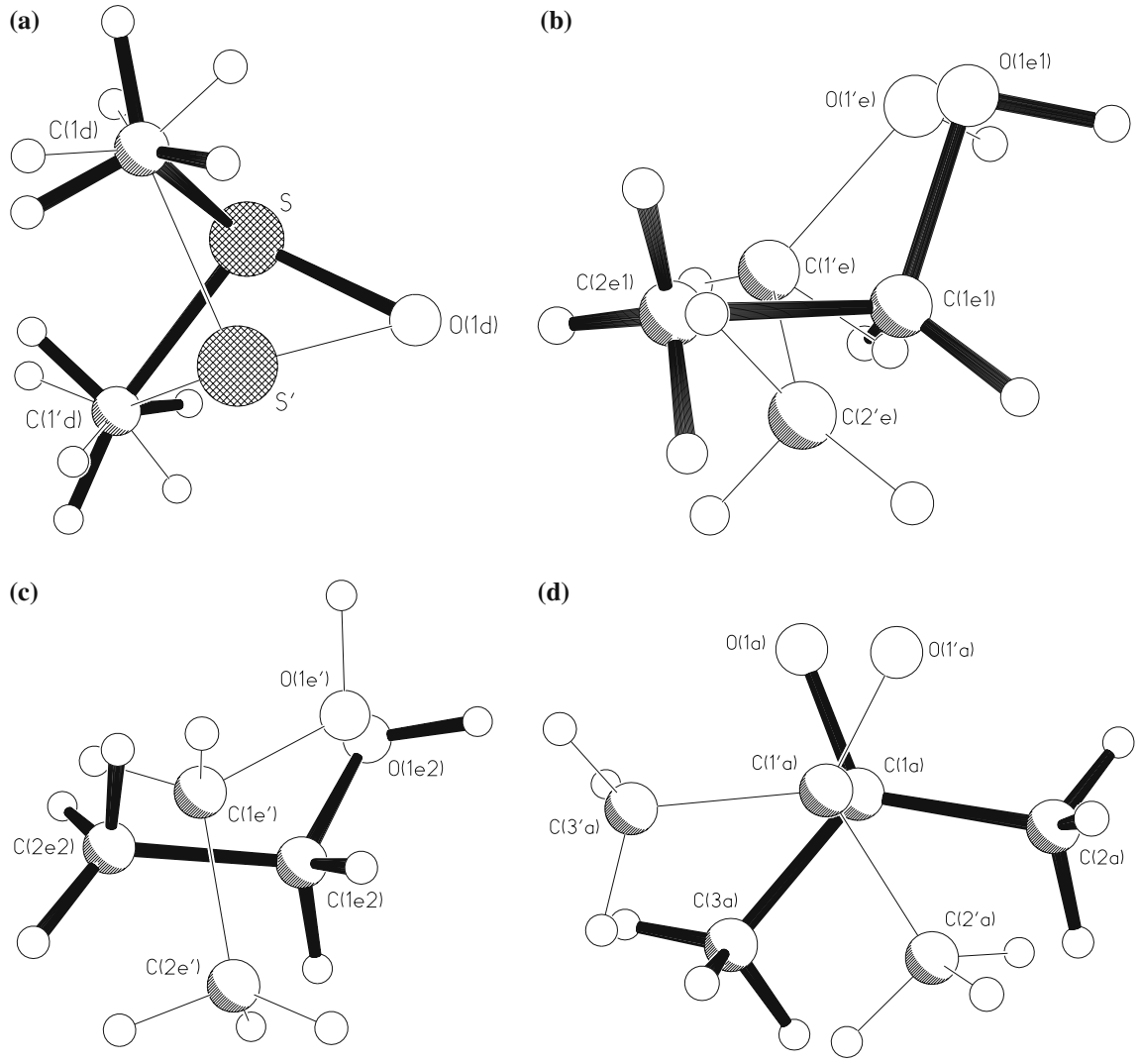

Figure 4. Continues on next page.

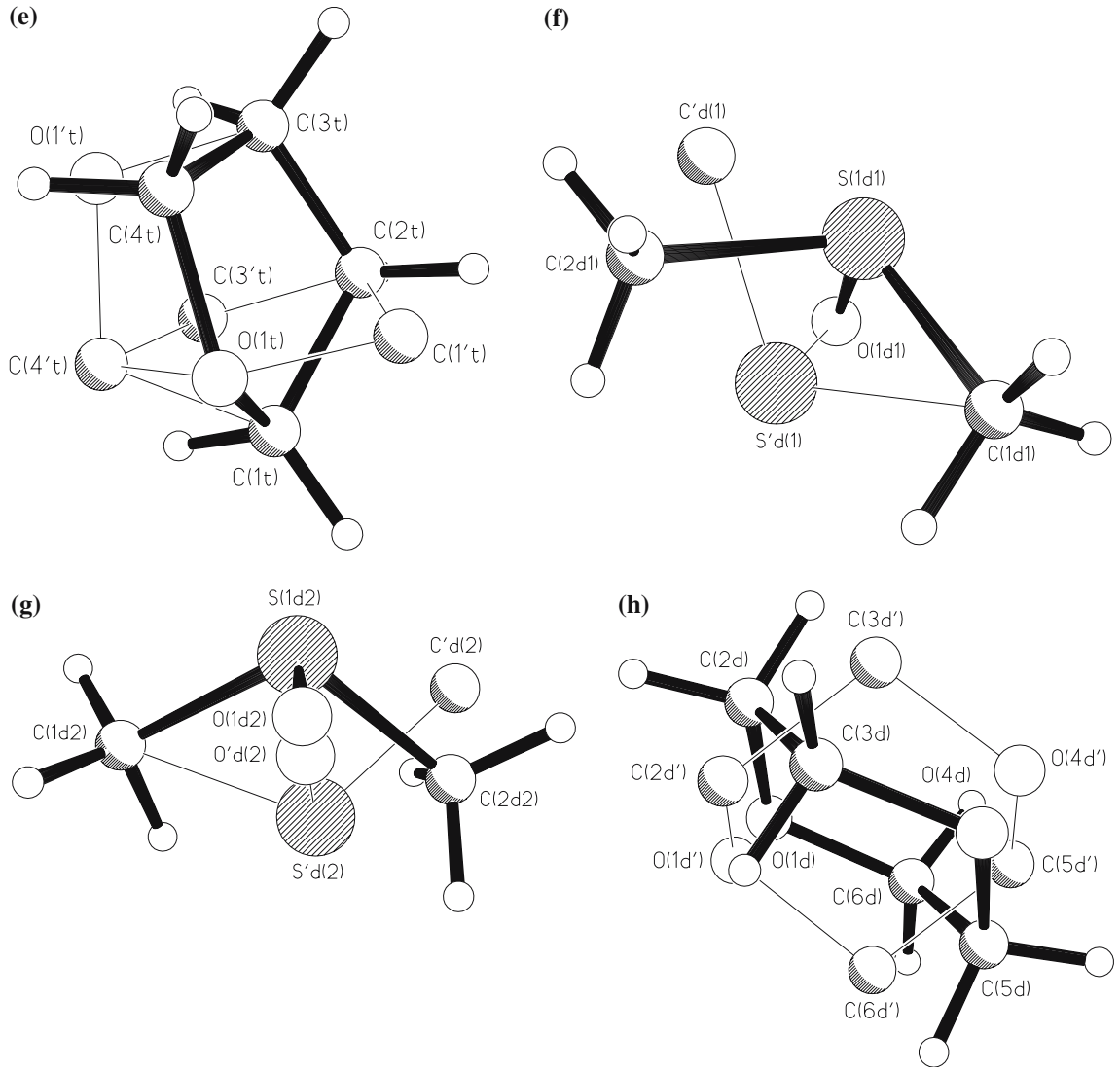

Figure 4. Perspective views of the guest molecules, exhibiting static disorder (with the major/minor site occupation factors given in parentheses), such as DMSO in **1**·DMSO (1:1) (0.50/0.50) (a); the two unique ethanol molecules in **3**·EtOH (1:1) (0.58/0.42) (b) and (0.55/0.45) (c); acetone in **3**·acetone (1:1) (0.54/0.46) (d); THF in **3**·THF (1:1) (∼0.7/∼0.2/∼0.1) (e); the two independent DMSO guests in **4**·DMSO (0.63/0.37) (1:1) (f) and (0.65/0.35) (g); and 1,4-dioxane in the **4**·dioxane (1:1) (0.75/0.25) (h) inclusion crystal. Unique non-hydrogen positions are labelled, and bonds to the minor disorder sites are indicated with thinner lines. In the case of **1**·DMSO (1:1) (a), where the two partly overlapping symmetry-related guest positions have equal probabilities (50%), bonds to the symmetry-generated S′ position and H sites to it are drawn with thinner lines. The minor H disorder sites with relatively low probabilities (sof < 0.40), such as those of the THF guest in **3**·THF (1:1) (e), of the DMSO molecules in **4**·DMSO (1:1) (f, g) and of the 1,4-dioxane in **4**·1,4-dioxane (1:1) (h), were not included in the final structure models (see the text).

remarkably different host:guest stoichiometries (4:1 and 1:1, respectively), although the guest recognition yields a closed loop of hydrogen bonds in both cases. Worth noting, however, are the different sizes and compositions of the H-bonded rings: the asymmetric closed loop of H-bonds [$\mathbf{R}\ ^{5}_{5}\mathbf{(10)}$] in **1**·EtOH (4:1) is created by five OH functions of four host molecules and one guest alcohol, whereas in **2**·MeOH (1:1) four OH groups, coming from two host and two guest molecules, form the centrosymmetric H-bonded ring with the graph descriptor [$\mathbf{R}\ ^{4}_{4}\mathbf{(8)}$]. These structural differences, however, hardly explain the observed dissimilarity in the ability of hosts **1** and **2** to enclathrate alcoholic guests (see above). Also the 1,4-dioxane inclusions of these two hosts [15] differ, not only in the host:guest stoichiometry [4:1 and 1:1] but also in the guest recognition and packing modes. Instead of a double-acceptor guest-molecule pattern, such as in **1**·1,4-dioxane (4:1), each guest in the **2**·1,4-dioxane (1:1) complex is involved in one H-bond connection only, in the latter case thus violating the 'maximum acceptor rule' [28, 36]. Concerning the DMSO complexes of hosts **1** [**1**·DMSO (2:1)] and **2** [**2**·DMSO (2:1)] [18], comparison of the crystal data suggests possible relations between them. Moreover, the guest recognition modes (double-acceptor guest-molecule pattern in both crystals) and the type of static disorder of the DMSO molecules resemble each other. The calculated cell similarity index, $\Pi = 0.0348$, and the isometricity descriptor of the host molecules, $I(\mathrm{m}) = 93.34\%$ (comparing all 20 host non-H atoms in each compound), also seem to support a close relationship. However, the isostructurality $I(\mathrm{s})$ index (based

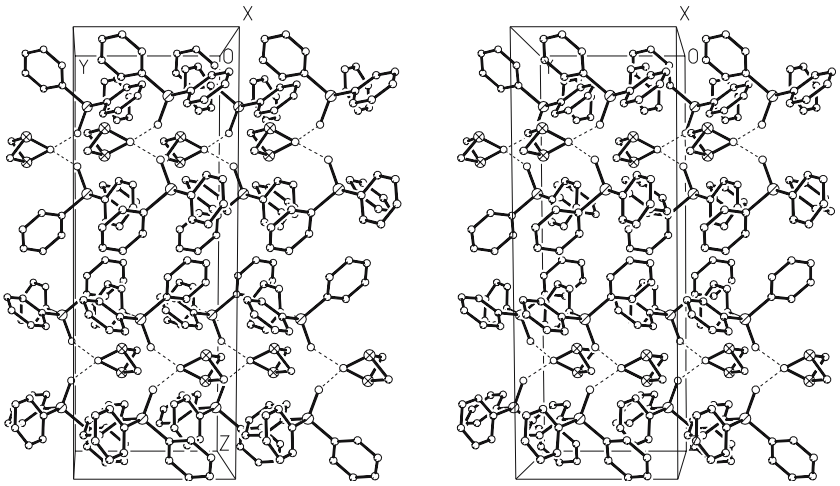

Figure 5. Stereo packing illustration of the **1**·DMSO (2:1) inclusion compound. H atoms are omitted for clarity, host–guest hydrogen bond interactions are indicated by dashed lines between the connected oxygen atoms. The DMSO guests are located in special positions, and each one occupies two partly overlapping disorder sites with equal probability.

only on the host skeletons) has the relatively low value 24.7%, thus implying significant differences between the host frameworks, and only low degree of homostructurality for these two DMSO inclusion compounds.

The related trinaphthyl-substituted silanol (**3**) and methanol (**4**) hosts proved to be highly superior in solid inclusion formation as compared to the phenyl-substituted ones, i.e. hosts **1** and **2** (cf. Tables 1 and 2). In the course of the present work, a total of ten crystalline complexes of the hosts **3** and **4** were studied [Table 3; Figures 2(a)–(f), 3(a)–(d) and 6–10], while crystal data of five additional inclusion compounds of

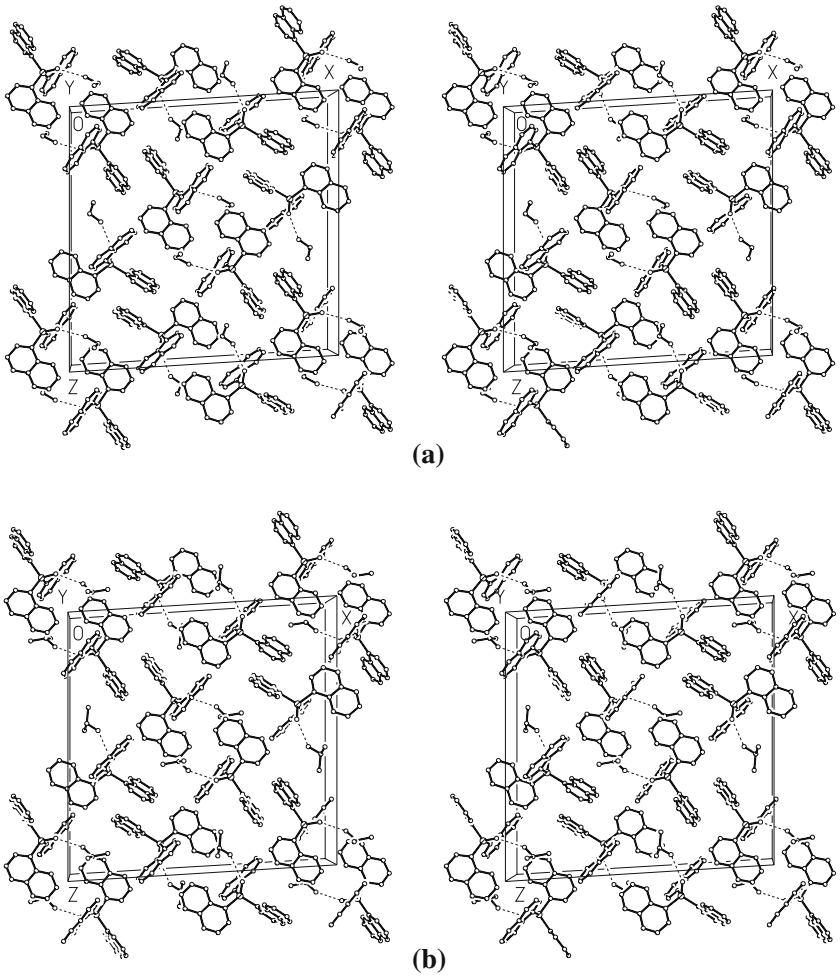

Figure 6. Stereo packing illustrations of the **3**·EtOH (1:1) (a) and **3**·*i*-PrOH (1:1) (b) inclusion compounds. Minor disorder sites in the ethanol molecules in (a), and the H atoms in both (a) and (b), are omitted for clarity. Host–guest H-bond interactions are indicated by dashed lines.

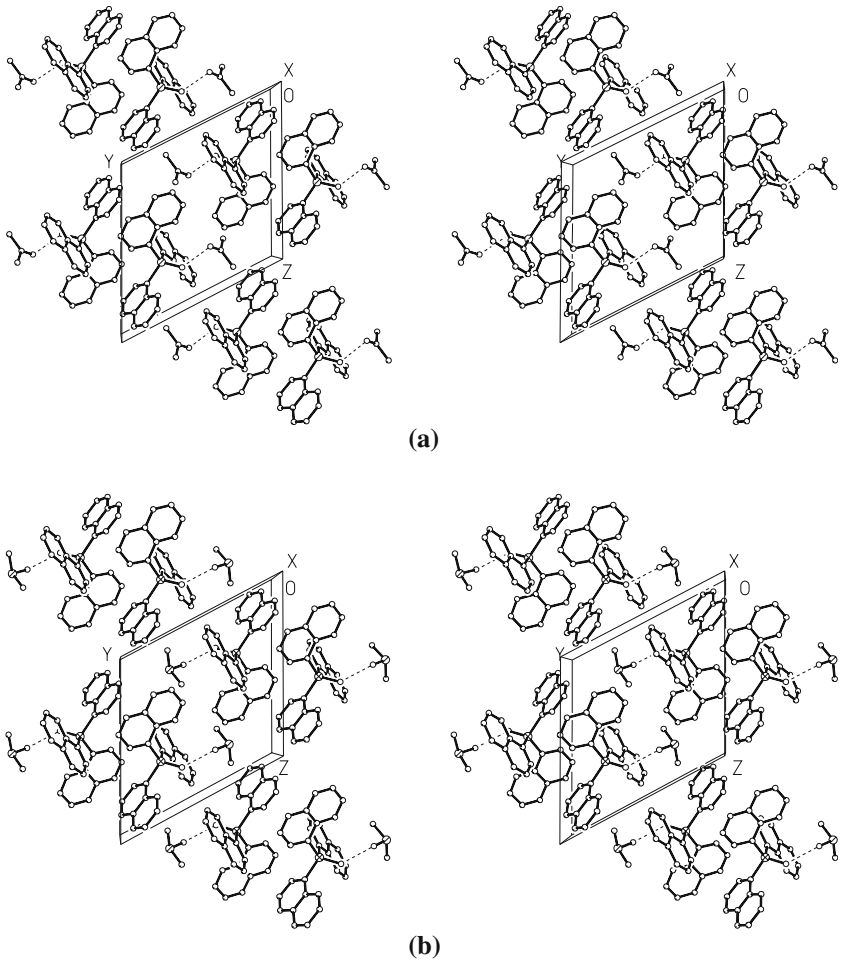

Figure 7. Stereo packing illustrations of the **3**·acetone (1:1) (a) and **3**·DMSO (1:1) (b) crystalline complexes. Minor guest disorder sites and the H atoms are omitted for clarity. Dashed lines indicate O(–H)···O hydrogen bond interactions.

host **3**, containing 1,4-dioxane [15], toluene, *o-, m-*, and *p*-xylene as guest [19], were taken from the literature [27].

Recognition of alcoholic guests by the naphthyl-substituted silanol host (**3**) did not yield a closed loop of hydrogen bonds, in all probability due to steric hindrance. Although no crystal structure of a solid alcoholic inclusion of host **4** is known to the authors, it seems likely that the bulkiness of the trinaphthyl substituents prevents the host OH functions from approaching each other to form rings of hydrogen bonds, as the triphenyl-substituted analogues (hosts **1** and **2**) do in their guest-free crystals [35, 37, 38] and alcoholic inclusion compounds [16, 18]. This suggestion is in accordance with our earlier experience involving various 9-substituted 9-fluorenol host compounds [39]. Instead of a coupled system of hydrogen bonds, each guest accepts a single H-bond from the nearest host OH function in the present ethanol and *i*-propanol inclusion compounds, just as the other polar guest molecules, such as acetone, DMSO, THF, piperidine and 1,4-dioxane [15] do in their co-crystals with host **3** (Figure 2(a)–(f), Table 4). As a consequence, the bulky host **3** forms 1:1 host–guest associates with each one of the above mentioned polar (protic or non-protic) guests, and this in turn leads to crystal formation with 1:1 host:guest ratio in all cases (Table 2). However, the crystal structures containing the protic and non-protic polar guests differ significantly from each other, as expressed by different crystal symmetries: the two alcoholic inclusion crystals are monoclinic, whereas those containing the non-protic polar guests (see above) are triclinic (Table 3). Furthermore, each of the crystals of **3**·EtOH (1:1) and **3**·*i*-PrOH (1:1) contains two symmetry-independent H-bonded host–guest associates, whereas only one such unit is to be found in the related co-crystals with the non-protic polar guests. At the same time, the two alcoholic inclusion compounds exhibit the same space group symmetry ($P2_1/n$), and have similar unit cell dimensions (Table 3) and packing arrangements (Figure 6), suggesting an intimate relationship between them. The host alcohol functions only as a proton donor, and the guest alcohol as an acceptor in both cases, thus creating structures without saturation of hydrogen bonds. The guest molecules are located in pocket-like (aediculate-type) [34] host arrangements in both crystals, yet each *i*-propanol guest occupies only one crystallographic site, whereas the allotted space makes static disorder possible for the smaller ethanol molecules (cf. Figure 4(b)–(c)). Calculation of the isostructurality descriptors [20, 21], comparing the two alcoholic

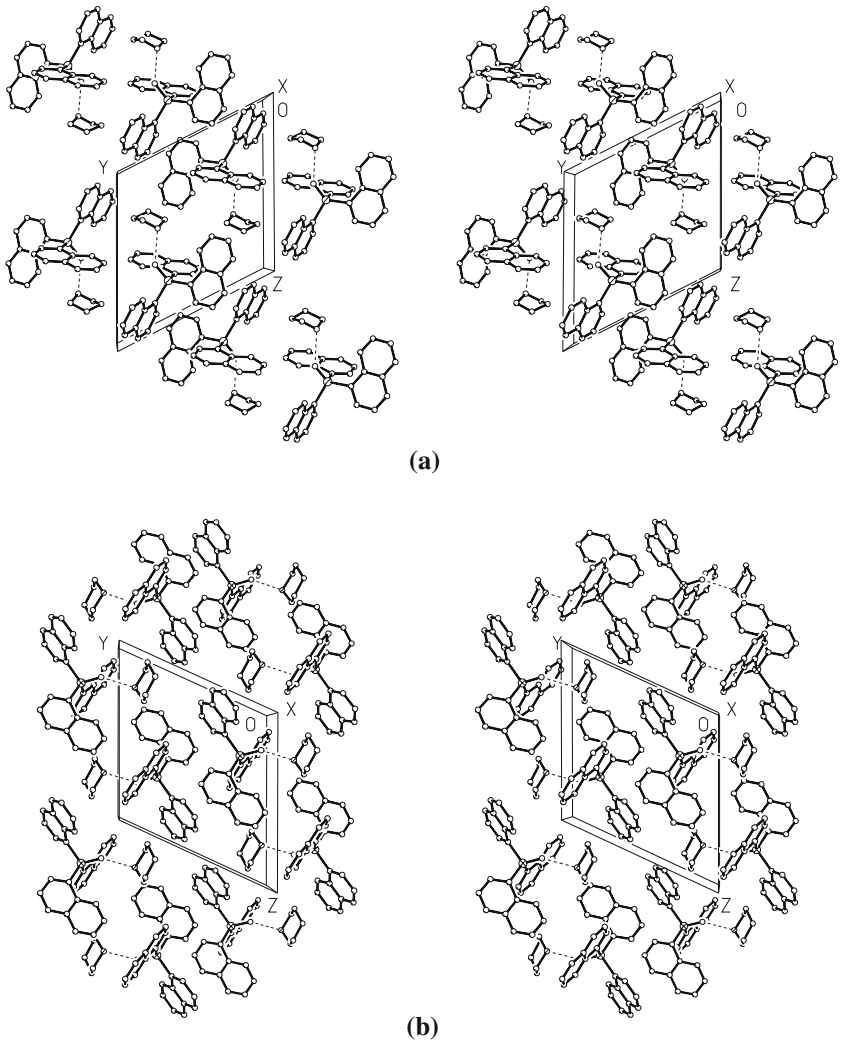

Figure 8. Stereo packing illustrations of the **3**·THF (1:1) (a) and **3**·piperidine (1:1) (b) crystalline complexes. Minor guest disorder sites in (a), and the H atoms in both (a) and (b) are omitted for clarity. Dashed lines indicate O–H···O hydrogen bond interactions.

inclusions of host **3**, yielded the values $\Pi = 0.00437$, $I(s) = 77.0\%$ and $I(m) = 99.675\%$, thus proving with good approximation a homostructural relationship between them. The isostructurality and isometricity indices of the host frameworks are based on the 64 non-hydrogen atom positions, which form the two unique host molecules in each inclusion crystal, i.e. in **3**·EtOH and **3**·*i*-PrOH, respectively.

Also crystals containing non-protic polar guests, such as **3**·acetone (1:1), **3**·DMSO (1:1), **3**·THF (1:1), **3**·piperidine (1:1) (Figures 7–8) and **3**·1,4-dioxane (1:1) [15], resemble each other due to identical crystal symmetry (triclinic, *P*-1), and similar shapes and sizes of the various H-bonded 1:1 host–guest units, i.e. the building blocks of the crystal structures. The different polar guests are included *via* hydrogen bond interaction with the silanol host (**3**) as proton donator (Table 4), and are located in the same pockets of the host frameworks. There are only weaker van der Waals type forces between the 1:1 host–guest associates. Calculations clearly indicate similar unit cells (cf. the Π values in Table 6) and almost identical conformation for the host **3** molecule in its different compounds [cf. the $I(m)$ values in Table 6]. The mean values of Π and $I(m)$ in Table 6 (with the root-mean-square deviations given in angular brackets) are 0.045[28] and 98.6[1.0]%, respectively. The isostructurality indices, $I(s)$, on the other hand, show wider scatter by ranging from 56.4 to 87.0% (Table 6) with an average value of 68[9]%. We may conclude from these results that all five co-crystals of host **3** containing non-protic polar guests (Table 6) are homostructurally related, though the degree of isostructurality varies appreciably among them.

Host–guest aggregates of 1:1 stoichiometric ratio were also observed in the co-crystals of host **3** with non-polar guests [19, 27] such as toluene (VOZJOJ), *o*-xylene (VOZJUP) and *m*-xylene (VOZKAW). In these latter cases the guest aryl π electrons function as acceptor of the hydrogen bond from the host OH function, forming (O)–H···π(aryl) host–guest interactions [40]. Due to the similar crystal building blocks, and the same triclinic (*P*-1) symmetry, the unit cell dimensions are also comparable in these compounds (Table 7), slightly resembling also the solid inclusion compounds of **3** cited

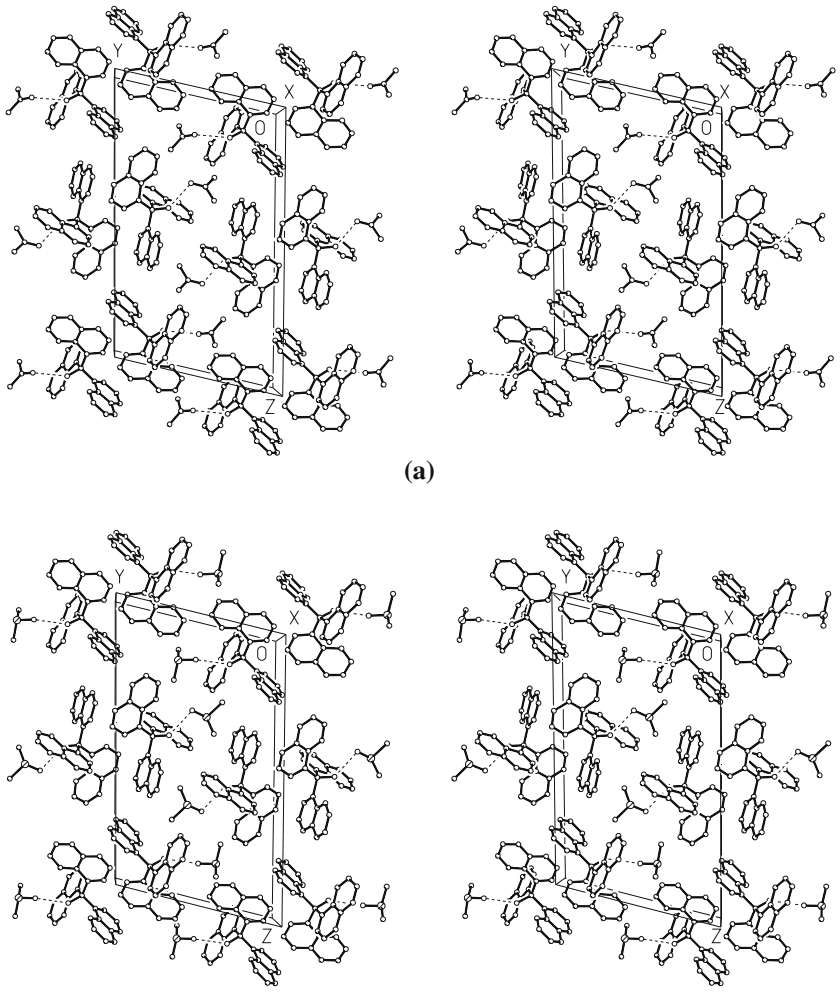

Figure 9. Stereo packing illustrations of the **4**·acetone (1:1) (a) and **4**·DMSO (1:1) (b) inclusion compounds. The minor disorder sites of the DMSO guest molecules in (b), and the hydrogen atoms in both (a) and (b) are omitted for clarity. Dashed lines indicate O(–H)···O hydrogen bond interactions.

above, containing non-protic polar guest molecules. However, despite this correspondence and similarity, the compared host frameworks within the cells do not overlap. Hence, the three structures of host **3** with the non-polar guests (i.e. toluene, *o*- and *m*-xylene [19]) have no isostructural relationship with each other. Interestingly enough, inclusion of the fourth non-polar guest, *p*-xylene, by host **3** yielded crystals with 1:2 host:guest stoichiometry, a different packing arrangement and increased unit cell dimensions (V_c = 1811.79 Å^3) [19, 27].

Also the four investigated solid inclusion compounds of the trinaphthyl-substituted methanol host **4** (Table 8) were found to exhibit the triclinic (*P*-1) crystal symmetry. In this latter case, however, inspection of the compositions of the crystallographic asymmetric units and the unit cell dimensions suggests that the **4**·acetone (1:1) and **4**·DMSO (1:1) complexes (Figure 9) make up one pair of related structures, whereas the **4**·1,4-dioxane (1:1) and **4**·benzene (1:1) co-crystals (Figure 10) may form another pair. As seen in Table 3, each of the acetone- and DMSO-containing crystals of **4** comprises two symmetry-independent H-bonded 1:1 host–guest associates (Figure 3(a)–(b)), whereas only one host and one guest constitute the unique part of the **4**·1,4-dioxane (1:1) or the **4**·benzene (1:1) co-crystals (Figure 3 (c)–(d)). The polar non-protic guests, such as acetone, DMSO and 1,4-dioxane, are included in the crystals *via* hydrogen-bond interaction from the carbinol host **4** to the respective guest (Table 4). On the other hand, no obvious H-bond type connection could be seen in the **4**·benzene (1:1) complex, contrary to the observations made in the toluene and *o*- or *m*-xylene inclusion compounds of the related silanol host **3** [19]. Though the host OH function seems to point in the direction of the adjacent benzene π electron systems also in the **4**·benzene (1:1) complex (Figure 10(b)), the calculated host–guest distances are relatively long: the O(1)···C(benzene) distances range between 3.84 and 4.23 Å, and those of H(1O)···C(benzene) are between 3.10 and 3.68 Å; the O(1)···π(benzene) and H(1O)···π(benzene) connections are 3.79 and 3.13 Å, respectively, and the O(1)–H(1O)···π(benzene) angle is 127°. These observations suggest only common van der Waals' type contacts between the benzene guest and the surrounding host **4**

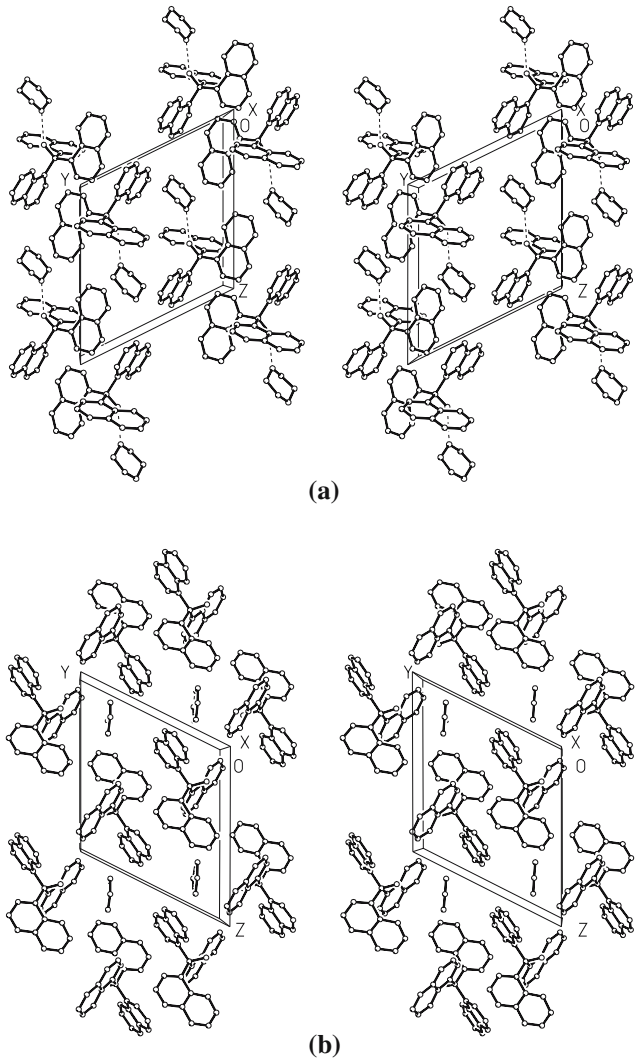

Figure 10. Stereo packing illustrations of the **4**·1,4-dioxane (1:1) (a) and **4**·benzene (1:1) (b) inclusion compounds. The hydrogen atoms, and the minor disorder C and O sites of the 1,4-dioxane molecule are omitted for clarity. The hydrogen bond between the host molecule and the 1,4-dioxane guest in (a) is indicated by a dashed line.

molecules, although the possibility of a weak O(H)···π host–guest interaction [40] can not be completely ruled out. Considering the calculated isostructurality indices (Table 8), they suggest a closer relationship for the pair of inclusion compounds with acetone and DMSO guests (both polar) than for the other pair, containing 1,4-dioxane (polar) and benzene (non-polar) as guest components.

Calculations were carried out in order to compare also related inclusion compounds of hosts **3** and **4**. In this connection, the crystal structures of three pairs of inclusion compounds have been investigated, in which identical guest molecules are included by hosts **3** and **4**, respectively, namely **3**·acetone (1:1) and **4**·acetone (1:1), **3**·DMSO (1:1) and **4**·DMSO (1:1), and **3**·1,4-dioxane (1:1) (JODYEG) [15, 27] and 4·1,4-dioxane (1:1). All these crystals have triclinic (*P*-1) symmetry and 1:1 host:guest stoichiometry. Nevertheless, the acetone and DMSO inclusion crystals of the carbinol host **4** contain not one but two symmetry independent 1:1 host:guest associates (Table 3, Figure 3(a) and (b)). Hence, these latter two co-crystals deviate considerably and are not comparable with the corresponding solid inclusion compounds of the silanol host **3** [i.e. **3**·acetone (1:1) and **3**·DMSO (1:1)]. On the other hand, inspection of space group symmetries, unit cell dimensions and compositions of the asymmetric units suggests that the 1,4-dioxane-containing compounds of the two hosts (**3** and **4**), and four more compounds, two with host **3** and two with host **4**, might be related. Therefore, isostructurality calculations [20, 21] were carried out, comparing the six crystal structures two by two. The results are listed in Table 9. The cell similarity descriptors, Π (with the average value 0.046[27]), are relatively low. The molecular isometricity indices, I(m) (with the mean value 95.2[1.8]%), imply that although the silanol Si atom is considerably bigger than the methanol carbon [r_{cov}(Si) $\approx$ 1.17 Å, r_{cov}(C) $\approx$ 0.77 Å] [41], the trinaphthyl-substituted silanol (**3**) and methanol (**4**) hosts exhibit a relatively high degree of isomorphism in the compared inclusion compounds. On the other hand, the low or modest values obtained for the isostructurality indices, I(s) (with a mean value of 29[15]%, Table 9), give evidence of significant variations in the host frameworks created by hosts **3** and **4**, even in the case of identical crystal symmetry and comparable unit cell dimensions (Scheme 1).

Conclusions

Previously documented host behaviour of the simple triarylmethanols **2** [15, 18] and **4** [17], as well as the extraordinary inclusion selectivity of triphenylsilanol (**1**) [16], prompted a more thorough study of the inclusion properties of the silanols **1** and **3** in comparison with the carbinol counterparts **2** and **4**. In summary of this study, the following conclusions can be drawn.

Replacement of the carbinol C-atoms in triarylmethanol hosts, of which **2** and **4** are classic examples, by silicon atoms to give the silanol analogues **1** and **3**, resulted in a distinct increase of the capability to form inclusion compounds with organic guests. This improvement is most obviously revealed by the rather broad formation of inclusion compounds of **1** with alcohols, which totally failed for the analogous carbinol **2**, except in the special case of the methanol inclusion compound of **2**. Similarly related, but far less pronounced are the compounds **3** and **4**, where the carbinol is also a little less efficient than the silanol. Moreover, the carbinol **4** compares somewhat unfavourably with the silanol **3** in the formation of inclusion compounds with amines. On the other hand, the ability to form inclusion compounds with dipolar aprotic and apolar guest solvents remains rather unaffected by the replacement of carbon by silicon.

X-ray diffraction studies and comparison of selected crystalline inclusion compounds of host molecules **1**-**4** with small organic guests showed a diversity of packing

Table 4. Distances and angles in O–H···O hydrogen bonds between host and guest, observed in inclusion compounds **1**·DMSO (2:1), **3**·EtOH (1s:1), **3**·*i*-PrOH (1:1), **3**·acetone (1:1), **3**·DMSO (1:1), **4**·acetone (1:1), **4**·DMSO (1:1) and **4**·1,4-dioxane (1:1)[a]

Atoms involved	Symmetry	O···O/N distance, Å	O–H distance, Å	H···O/N distance, Å	O-H···O/N angle, deg
1·DMSO (2:1)					
O(1)–H(1O)···O(1D)	*x*, *y*, *z*	2.757(2)	0.86	1.90	174
3·EtOH (1:1)					
O(1)–H(1O)···O(1E1)	*x*, *y*, *z*	2.80(1)	1.02	1.78	161
O(1)–H(1O)···O(1'E)	*x*, *y*, *z*	2.71(2)	1.02	1.73	159
O(1′)–H(1O′)···O(1E2)	*x*, *y*, *z*	2.79(1)	1.00	1.81	167
O(1′)–H(1O′)···O(1E2)	*x*, *y*, *z*	2.72(1)	1.00	1.72	177
3·i-PrOH (1:1)					
O(1)–H(1O)···O(1P1)	*x*, *y*, *z*	2.738(3)	0.93	1.82	168
O(1′)–H(1O')···O(1P2)	*x*, *y*, *z*	2.715(3)	0.95	1.77	171
3·acetone (1:1)					
O(1)–H(1O)···O(1A)	*x*, *y*, *z*	2.777(7)	0.94	1.84	174
O(1)–H(1O)···O(1′A)	*x*, *y*, *z*	2.731(9)	0.94	1.83	160
3·DMSO (1:1)					
O(1)–H(1O)···O(1D)	*x*, *y*, *z*	2.668(4)	0.97	1.71	170
3·THF (1:1)					
O(1)–H(1O)···O(1T)	*x*, *y*, *z*	2.707(3)	0.83	1.87	178
3·piperidine (1:1)					
O(1)–H(1O)···N(1P)	*x*, *y*, *z*	2.719(3)	0.93	1.80	172
4·acetone (1:1)					
O(1)–H(1O)···O(1A1)	*x*, *y*, *z*	2.830(3)	0.94	1.90	167
O(1′)–H(1O')···O(1A2)	*x*, *y*, *z*	2.849(4)	0.9	1.99	160
4·DMSO (1:1)					
O(1)–H(1O)···O(1D1)	*x*, *y*, *z*	2.740(3)	0.97	1.83	155
O(1′)–H(1O′)···O(1D2)	*x*, *y*, *z*	2.756(4)	0.94	1.90	151
O(1′)–H(1O′)···O(′D2)	*x*, *y*, *z*	2.778(9)	0.94	1.88	159
4·1,4-dioxane (1:1)					
O(1)–H(1O)···O(1D)	*x*, *y*, *z*	2.775(3)	0.97	1.86	157
O(1)–H(1O)···O(1D')	*x*, *y*, *z*	2.812(8)	0.97	1.94	149

[a]Esd's, where given, are in parentheses. The (O–)H positions were deduced from difference electron density maps, and were held riding on the respective parent oxygen atom during the subsequent calculations. Distances and angles were calculated without normalization of the H atom positions.

arrangements, but also pronounced similarities. The triphenyl-substituted host molecules **1** and **2**, on the one hand, and the trinaphthyl-substituted hosts **3** and **4**, on the other hand, exhibit a high or very high degree of molecular isomorphism in the different compounds studied, thus indicating limited variability for the host skeletons. The host OH functions play a crucial role in the guest recognition and inclusion processes for all four hosts **1**–**4** by establishing H-bond interactions with the various guests whenever possible. However, only the triphenyl-substituted methanol/silanol hosts are known to self-associate into cyclic tetramers through O-H···O hydrogen bonds, and in this way form crystal structures also on their own [35, 37, 38]. By contrast, the voluminous trinaphthyl group seems to prevent hosts **3** and **4** from establishing shorter, directional host–host interactions and/or coupled systems of hydrogen bonds, though both these latter hosts proved to be better in inclusion formation also with alcoholic guests, than the related triphenyl-substituted hosts **1** and **2**. These observations can probably be rationalized by suggesting that the superior clathrate formation ability of hosts **3**

Table 5. Comparison of related co-crystals of the triphenyl methanol host **2**[a,b]

Structure 1 (CCDC code)	Structure 2 (CCDC code)	Cell similarity index, Π[a]	No. of atoms compared	Molecular isometricity index, *I*(m) [%][a]
2·acetone(2:1) (JARRUP02)	**2**·DMSO(2:1) (JARROJ)	0.0122	20	69.99
2·dioxane (1:1) (JODXUV)	**2**·MeOH (1:1) (JARRID)	0.0017	20	73.28

[a]Following A. Kálmán *et al*. [20, 21].
[b]Data from the literature [15, 17, 18, 27].

Table 6. Comparison of four analogous inclusion compounds of the trinaphthyl silanol host **3** containing non-protic polar guests

Structure 1	Structure 2	Cell similarity index, Π[a]	Isostructurality index, *I*(s) [%][a, b]	Molecular isometricity index, *I*(m) [%][a, b]
3·acetone (1:1)	**3**·DMSO (1:1)	0.0201	70.3	99.61
3·acetone (1:1)	**3**·THF (1:1)	0.0317	71.3	99.56
3·acetone (1:1)	**3**·piperidine (1:1)	0.0833	59.1	98.75
3·DMSO (1:1)	**3**·THF (1:1)	0.0115	87.0	99.59
3·DMSO (1:1)	**3**·piperidine (1:1)	0.0620	56.4	99.12
3·THF (1:1)	**3**·piperidine (1:1)	0.0500	60.1	98.85
3·1,4-dioxane (1:1)[c]	**3**·acetone (1:1)	0.0792	62.3	97.63
3·1,4-dioxane (1:1)[c]	**3**·DMSO (1:1)	0.0607	64.8	97.10
3·1,4-dioxane (1:1)[c]	**3**·THF (1:1)	0.0499	70.6	97.15
3·1,4-dioxane (1:1)[c]	**3**·piperidine (1:1)	0.0025	74.0	99.08

[a]Following A. Kálmán *et al*. [20, 21].
[b]The isostructurality and the molecular isometricity indices were calculated for the 32 non-hydrogen atoms of the host molecule in each compound.
[c]From ref. [15] (CCDC code: JODYEG) [27].

Table 7. Comparison of the unit cell dimensions of three crystalline inclusion compounds of host **3** containing non-polar guests

Crystal 1 (CCDC code)	Crystal 2 (CCDC code)	Unit cell volume Crystal 1/Crystal 2 [Å^3]	Cell similarity index, Π[a]
3·toluene (1:1)[b] (VOZJOJ)	**3**·*o*-xylene (1:1)[b] (VOZJUP)	1405.52/1429.06	0.0172
3·toluene (1:1)[b] (VOZJOJ)	**3**·m-xylene (1:1)[b] (VOZKAW)	1405.52/1432.87	0.1586
3·*o*-xylene (1:1)[b] (VOZJUP)	**3**·m-xylene (1:1)[b] (VOZKAW)	1429.06/1432.87	0.1439

[a]Following A. Kálmán *et al*. [20, 21].
[b]Data from the literature [19, 27].

Table 8. Comparison of related co-crystals of the trinaphthyl methanol host **4**

Structure 1	Structure 2	Cell similarity index, Π [a]	No. of atoms compared	Isostructurality index, *I*(s) [%][a]	Molecular isometricity index, *I*(m) [%][a]
4·acetone (1:1)	**4**·DMSO (1:1)	0.0325	64	61.1	99.61
4·dioxane (1:1)	**4**·benzene (1:1)	0.0200	32	41.5	95.95

[a]Following A. Kálmán *et al*. [20, 21].

Table 9. Comparison of the host frameworks formed by hosts **3** and **4** in selected inclusion compounds

Structure 1	Structure 2	Cell similarity index, Π[a]	No. of atoms compared	Isostructurality index, *I*(s) [%][a]	Molecular isometricity index, *I*(m) [%][a]
3·acetone (1:1)	**4**·1,4-dioxane (1:1)	0.0615	32	25.9	97.21
3·acetone (1:1)	**4**·benzene (1:1)	0.0827	32	4.0	93.46
3·DMSO (1:1)	**4**·1,4-dioxane (1:1)	0.0406	32	42.4	97.23
3·DMSO (1:1)	**4**·benzene (1:1)	0.0614	32	22.0	93.25
3·1,4-dioxane (1:1)[b]	**4**·1,4-dioxane (1:1)	0.0226	32	39.2	95.53
3·1,4-dioxane (1:1)[b]	**4**·benzene (1:1)	0.0117	32	41.7	94.57

[a]Following A. Kálmán *et al*. [20, 21].
[b]From ref. [14] (CCDC code: JODYEG) [27].

and **4** in relation to the smaller hosts **1** and **2** is a consequence of the bulkiness of the former molecules, which in turn makes inclusion of small guest molecules a necessity for formation of dense packing and stable crystal structures by the trinaphthyl-substituted hosts [5b, 9]. At the same time, substitution of the central carbon atom by silicon may affect the clathrate formation ability through possible electronic effects, since the C↔Si exchange gives rise only to a minor increase of the host dimensions [14]. Thus, the observed specific behaviour of the silanol functional group relative to the carbinol structural unit opens up a new possibility for the design of highly selective crystalline host compounds.

Acknowledgements

E.W. gratefully acknowledges financial support from the Deutsche Forschungsgemeinschaft (SPP 472) and the Fonds der Chemischen Industrie.

Supplementary Data relevant to this publication have been deposited with the Cambridge Crystallographic Data Centre as supplementary publications nos. CCDC 274780–274790.

References

1. E. Weber: In J.J. Kroschwitz (ed.), *Kirk-Othmer Encyclopedia of Chemical Technology*, Wiley New York, 4th edn. suppl. (1998), 352 pp.
2. J.L. Atwood, J.E.D. Davies, and D.D. MacNicol (eds): *Inclusion Compounds* Vol. 4 and 5, Oxford University Press, Oxford (1991).
3. J.W. Steed and J.L. Atwood: *Supramolecular Chemistry*, Wiley, Chichester (2000).
4. D.D. MacNicol, F. Toda, and R. Bishop (eds): *Comprehensive Supramolecular Chemistry* Vol. 6, Elsevier, Oxford (1996).
5. (a) F. Toda: In Ref. 2, Vol. 4, 126 pp. (b) E. Weber: In Ref. 4, 535 pp.
6. F. Toda and R. Bishop (eds): *Separations and Reactions in Organic Supramolecular Chemistry, Perspectives in Supramolecular Chemistry* Vol. 8, Wiley, Chichester (2004).
7. (a) R. Bishop: *Chem. Soc. Rev.* 311 (1996). (b) E. Weber: In E. Weber (ed.), *Molecular Inclusion and Molecular Recognition – Clathrates I, Topics in Current Chemistry*, Vol. 140, Springer-Verlag, Berlin, Heidelberg (1987), 1 pp.
8. G.R. Desiraju: In Ref. 4, 1 pp.
9. E. Weber, M. Czugler: In E. Weber, (ed.), *Molecular Inclusion and Molecular Recognition – Clathrates II, Topics in Current Chemistry*, Vol. 149, Springer-Verlag, Berlin, Heidelberg (1988), pp. 45.
10. (a) E. Weber: In Ref. 2, Vol. 4, 188 pp. (b) K. Beketov, E. Weber, B.T. Ibragimov, J. Seidel and K. Köhnke: *Adv. Mater.* **12**, 664 (2000).
11. (a) I. Csöregh and E. Weber: In A.W. Coleman (ed.), *Molecular Recognition and Inclusion*, Kluwer, Dordrecht (1998), 301 pp. (b) I. Csöregh, E. Weber, and T. Hens: *J. Incl. Phenom.* **38**, 397 (2000).
12. (a) P. Dastidar and I. Goldberg: In Ref. 4, 305 pp. (b) P. Finocchiaro and S. Failla: In Ref. 4, 593 pp.
13. (a) T. Müller, J. Hulliger, W. Seichter, E. Weber, T. Weber, and M. Wübbenhorst: *Chem. Eur. J.* **6**, 54 (2000). (b) E. Weber, P.P. Korkas, M. Czugler, and W. Seichter: *Supramol. Chem.* **16**, 217 (2004).
14. S.I. Nitsche, E. Weber, W. Seichter, N. Báthori, K.M. Beketov, and G. Roewer: *Silicon Chem.* **2**, 55 (2003).
15. S.A. Bourne, L. Johnson, C. Marais, L.R. Nassimbeni, E. Weber, K. Skobridis, and F. Toda: *J. Chem. Soc., Perkin Trans.* **2**, 1707 (1991).
16. S.A. Bourne, L.R. Nassimbeni, K. Skobridis, and E. Weber: *J. Chem. Soc., Chem. Commun.* 282 (1991).
17. E. Weber, K. Skobridis, A. Wierig, and I. Goldberg: *J. Incl. Phenom.* **28**, 163 (1997).
18. E. Weber, K. Skobridis, and I. Goldberg: *J. Chem. Soc., Chem. Comm.* 1195 (1989).
19. S.A. Bourne, L.R. Nassimbeni, E. Weber, and K. Skobridis: *J. Org. Chem.* **57**, 2438 (1992).
20. A. Kálmán, L. Párkányi, and G. Argay: *Acta Crystallogr. Sect. B* **49**, 1039 (1993).
21. A. Kálmán and L. Párkányi: Isostructurality of organic crystals, in M. Hargittai and I. Hargittai (eds.), *Advances in Molecular Structure Research*, Vol. 3, JAI Press Inc. (1997), pp. 189–226.
22. STOE & CIE GmbH, 1997 (Publications 4805-014).
23. A.L. Spek: *HELENA, Program for Data Reduction*, University of Utrecht, The Netherlands (1993).
24. G.M. Sheldrick: *SHELX 97, Program for Crystal Structure Solution*, University of Göttingen, Germany (1997).
25. J. Schmidlin and P. Massini: *Ber. Dtsch. Chem. Ges.* **42**, 2397 (1909).
26. K. Skobridis, E. Weber, and W. Seichter: *Z. Kristallogr. NCS* **218**, 469 (2003).
27. F.H. Allen and W.D.S. Motherwell: *Acta Crystallogr. Sect. B* **58**, 407 (2002); CCDC Database, Version 5.26 (November 2004).
28. M.C. Etter: *Acc. Chem. Res.* **23**, 120 (1990).
29. J. Bernstein, R. Davis, L. Shimoni, and N.-L. Chang: *Angew. Chem. Int. Ed.* **34**, 1555 (1995)(and references therein).
30. I. Csöregh, T. Brehmer, S.I. Nitsche, W. Seichter, and E. Weber: *J. Incl. Phenom.* **47**, 113 (2003).
31. E. Weber, S. Nitsche, A. Wierig, and I. Csöregh: *Eur. J. Org. Chem.* , 856 (2002).
32. I. Csöregh, A. Sjögren, M. Czugler, M. Cserzö, and E. Weber: *J. Chem. Soc. Perkin Trans.* **2**, 507 (1986).
33. T.H. Brehmer, R. Kirchner, J. Seidel, and E. Weber: *J. Phys. Org. Chem.* **15**, 270 (2002).
34. E. Weber and H.-P. Josel: *J. Incl. Phenom.* **1**, 79 (1983).
35. K.F. Bowes, C. Glidewell, and J.N. Low: *Acta Crystallogr. Sect. C.* **58**, 409 (2002).
36. M.C. Etter: *J. Phys. Chem.* **95**, 4601 (1991).
37. H. Puff, K. Braun, and H. Reuter: *J. Organomet. Chem.* **409**, 119 (1991).
38. G. Ferguson, J.F. Gallagher, C. Glidewell, J.N. Low, and S.N. Scrimgeour: *Acta Crystallogr.* **Sect. C48**, 1272 (1992).
39. I. Csöregh, M. Czugler, and E. Weber: *J. Phys. Org. Chem.* **6**, 171 (1993).
40. G.R. Desiraju and T. Steiner: *The Weak Hydrogen Bond, IUCr Monographs on Crystallography,* Vol. 9, Oxford University Press, Oxford (1999).
41. A.J.C. Wilson (ed): *International Tables for Crystallography,* Vol. C, Kluwer Academic Publishers, Dordrecht, Boston, London (1995), pp. 692–706.